

Lattice dynamics of hcp Ti

C. Stassis, D. Arch, and B. N. Harmon

Ames Laboratory—U.S. Department of Energy and Department of Physics, Iowa State University, Ames, Iowa 50011

N. Wakabayashi

Solid State Division, Oak Ridge National Laboratory, Oak Ridge, Tennessee 37830

(Received 31 July 1978)

Inelastic-neutron-scattering techniques have been used to study the lattice dynamics of hcp Ti. The phonon dispersion curves along the [001], [100], and [110] symmetry directions were determined at 295, 773, and 1054 K. As the temperature decreases, we observe a rather large increase in the frequencies of all but the [001]LO branch. The zone-center mode of the [001]LO branch softens appreciably and at room temperature this branch exhibits a dip at the zone center. These features of the phonon spectrum of hcp Ti bear a striking resemblance to those of hcp Zr and seem to be characteristic of the transition metals of column IV of the Periodic Table. The data were used to evaluate the lattice specific heat at constant pressure as a function of temperature. The calculated total specific heat, obtained by taking into account the electronic contribution, was found to agree, to within experimental uncertainties, with the results of direct specific-heat measurements.

I. INTRODUCTION

In recent years, considerable effort has been directed towards an understanding of the electron-phonon interaction and its effect on a wide variety of phenomena in solids. Of course, one of the most immediate manifestations of the electron-phonon interaction is the effect on the lattice dynamics itself. As a result the lattice dynamics of superconducting elements, in which the electron-phonon interaction is expected to be strong, has been the subject of many theoretical and experimental investigations. Of particular interest is a detailed understanding of the lattice dynamics of superconducting transition elements and their compounds. These metals exhibit rather strong anomalies in their phonon spectra whose origin is generally attributed to the strong electron-phonon interaction in these metals. The transition elements in the fifth and sixth columns of the Periodic Table, and in particular Nb, have been extensively studied since the experiments and their interpretations are considerably simplified by the fact that these elements have the same crystal structure: body-centered cubic. The transition elements of the fourth column, on the other hand, have not received as much attention because, although they solidify to a bcc structure (β phase), all undergo, at temperatures below 1000 K, a transformation of the martensitic variety to the hcp structure (α phase).

The lattice dynamics of the transition elements of the fourth column of the Periodic Table is also of interest in connection with the electrical and

thermodynamical properties of these metals which exhibit some rather remarkable features at high temperatures. The electrical resistivity¹ at high temperatures nearly saturates to a constant value and the heat capacity² at constant pressure for the hcp phase increases more rapidly with increasing temperature than one would expect from a simple consideration of anharmonic and electronic corrections to the Dulong-Petit law.

We initiated therefore a systematic study of the lattice dynamics of these elements in both the α and β phases using inelastic-neutron-scattering techniques. In these studies the dispersion curves as well as their temperature dependence are investigated in order to obtain information about the temperature dependence of the thermophysical properties of these elements as well as the change with temperature of the electronic response to the nuclear motions.

The experimental results for hcp Zr have been given in a previous paper,³ hereafter referred to as I. In the present paper we present the results of an investigation of the lattice dynamics of hcp Ti. We find that the main features of the lattice dynamics of hcp Ti are similar to those of hcp Zr. In particular we observe a relatively large decrease with increasing temperature in the frequencies of all but the [001]LO branch. The zone-center mode of the [001]LO branch softens appreciably with decreasing temperature and at room temperature this branch exhibits a dip at the zone center, a behavior similar to that observed in hcp Zr. The data were used to calculate the lattice specific heat at constant pressure which, combined

with a band-theoretical calculation of the electronic specific heat, can account for the observed temperature dependence of the total specific heat of Ti.

II. EXPERIMENTAL DETAILS

The crystals used in the present experiment were prepared from high purity Ti obtained from the Titanium Metal Co. Large single crystals of hcp Ti (3–4 cm³) were grown by the same technique used in the preparation of the hcp Zr crystals (see I). The measurements were performed using a vacuum furnace (described in I) mounted on the sample goniometer of a triple-axis spectrometer. At the highest temperature reached in the experiments the temperature was controlled to within a few degrees and the vacuum was approximately 10⁻⁵ Torr.

The measurements were performed using a triple-axis spectrometer at the High Flux Isotope Reactor of the Oak Ridge National Laboratory. All data were collected with the spectrometer in the constant Q method of operation (where Q denotes the neutron scattering vector). A fixed incident energy of 14.75 meV was used and neutron groups scattered with energy gain were detected. Pyrolytic graphite was used as a monochromator and analyzer and a pyrolytic graphite filter was placed in the incident beam to attenuate higher-order contaminations. At each temperature the lattice constants of the crystal were assessed by determining the scattering angle of selected Bragg reflections and were found to be in agreement with thermal-expansion measurements.⁴

III. EXPERIMENTAL RESULTS

The phonon dispersion curves, along the [001], [100], and [110] symmetry directions, were determined at 295, 773, and 1054 K. The measured phonon frequencies are listed in Table I and the experimental dispersion curves are plotted in Figs. 1 and 2. The room-temperature data are in general agreement with previous measurements of the dispersion curves by one of the authors (N. W.).

A. General characteristics

It can be seen from Table I and Fig. 2 that the frequencies of all but the [001]LO branch decrease with increasing temperature. This behavior is similar to that observed in hcp Zr (see Figs. 2 and 3 of I); actually the observed relative frequency changes with varying temperature are approximately of the same magnitude. This temperature dependence is what one would expect from the normal

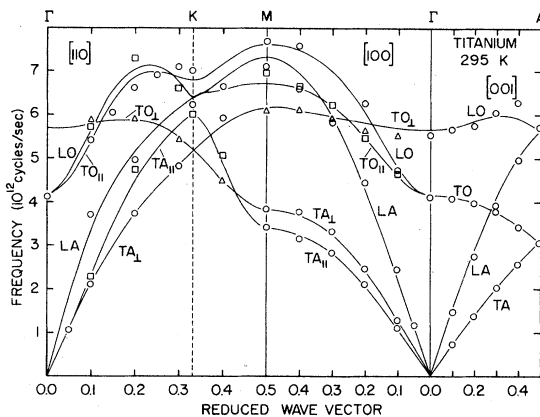


FIG. 1. Phonon dispersion curves of hcp Ti along the [001], [100], and [110] symmetry directions at 295 K. The solid lines were obtained by fitting the data to the force constant model of DeWames *et al.* (Ref. 12.).

volume dependence of the phonon frequencies. However, the frequency shifts due to this effect, estimated using the thermodynamic Grüneisen parameter,⁵ are much smaller than those experimentally observed. Thus, the observed frequency shifts are mainly due to an explicit temperature

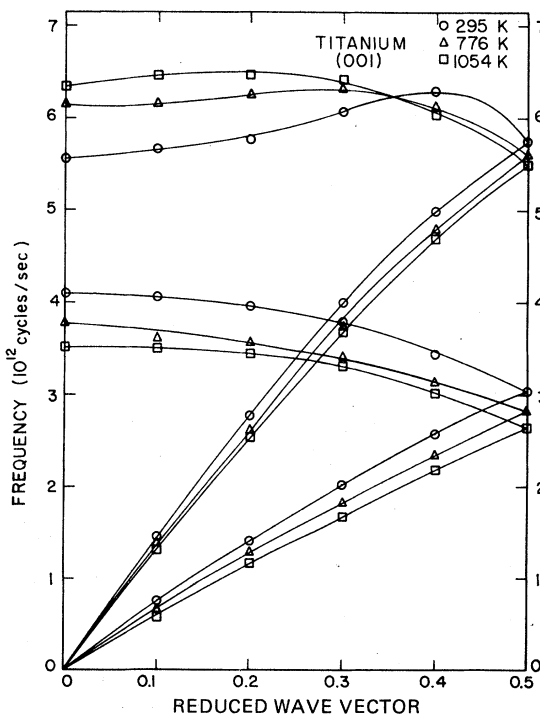


FIG. 2. Temperature dependence of the dispersion curves of hcp Ti along the [001] direction.

TABLE I. Measured frequencies (THz) of hcp Ti. The symbols \perp and \parallel refer to polarizations perpendicular and parallel to the basal plane, respectively.

ξ	$T = 295$ K	$T = 773$ K	$T = 1054$ K	ξ	$T = 295$ K	$T = 773$ K	$T = 1054$ K
TA [00 ξ]				TO $_{\parallel}$ [ξ 00]			
0.1	0.74 \pm 0.03	0.66 \pm 0.02	0.57 \pm 0.02	0.1	4.64 \pm 0.08	4.21 \pm 0.06	4.03 \pm 0.06
0.2	1.38 \pm 0.03	1.26 \pm 0.03	1.16 \pm 0.02	0.2	5.45 \pm 0.04	5.03 \pm 0.06	4.83 \pm 0.05
0.3	2.03 \pm 0.03	1.83 \pm 0.03	1.68 \pm 0.02	0.3	6.24 \pm 0.06	6.04 \pm 0.12	
0.4	2.56 \pm 0.03	2.36 \pm 0.02	2.19 \pm 0.04	0.4	6.62 \pm 0.08	6.4 \pm 0.2	6.42 \pm 0.04
0.5	3.05 \pm 0.03	2.81 \pm 0.08	2.63 \pm 0.04	0.5	6.95 \pm 0.12	6.82 \pm 0.12	6.73 \pm 0.1
TO [00 ξ]				LO [ξ 00]			
0.0	4.1 \pm 0.15	3.77 \pm 0.12	3.53 \pm 0.12	0.1	4.7 \pm 0.06
0.1	4.07 \pm 0.15	3.6 \pm 0.05	3.5 \pm 0.06	0.15	...	5.07 \pm 0.06	4.7 \pm 0.05
0.2	3.95 \pm 0.10	3.54 \pm 0.05	3.45 \pm 0.08	0.2	6.26 \pm 0.04	5.7 \pm 0.06	5.4 \pm 0.04
0.3	3.79 \pm 0.05	3.40 \pm 0.05	3.31 \pm 0.04	0.25	...	6.2 \pm 0.06	5.92 \pm 0.1
0.4	3.43 \pm 0.05	3.13 \pm 0.06	3.0 \pm 0.06	0.4	7.59 \pm 0.04	7.1 \pm 0.03	6.8 \pm 0.1
LA [00 ξ]				0.5	7.69 \pm 0.04
0.1	1.45 \pm 0.05	1.34 \pm 0.03	1.33 \pm 0.04	TA $_{\perp}$ [$\xi\xi$ 0]			
0.2	2.74 \pm 0.06	2.61 \pm 0.03	2.55 \pm 0.04	0.05	1.07 \pm 0.04	0.95 \pm 0.04	0.88 \pm 0.04
0.3	3.91 \pm 0.05	3.77 \pm 0.08	3.69 \pm 0.06	0.1	2.1 \pm 0.03	1.88 \pm 0.02	1.74 \pm 0.02
0.4	4.97 \pm 0.06	4.79 \pm 0.04	4.67 \pm 0.06	0.2	3.7 \pm 0.04	3.45 \pm 0.03	3.32 \pm 0.04
0.5	5.73 \pm 0.05	5.59 \pm 0.04	5.50 \pm 0.06	0.3	4.82 \pm 0.06	4.8 \pm 0.15	4.64 \pm 0.06
LO [00 ξ]				0.4	5.93 \pm 0.04		
0	5.54 \pm 0.15	6.14 \pm 0.15	6.33 \pm 0.2	LA [$\xi\xi$ 0]			
0.1	5.67 \pm 0.15	6.13 \pm 0.12	6.44 \pm 0.12	0.1	3.7 \pm 0.08	3.32 \pm 0.09	3.04 \pm 0.05
0.2	5.75 \pm 0.20	6.24 \pm 0.10	6.46 \pm 0.1	0.2	4.96 \pm 0.08	4.69 \pm 0.04	4.28 \pm 0.04
0.3	6.06 \pm 0.20	6.31 \pm 0.10	6.40 \pm 0.2	0.33	6.23 \pm 0.03		
0.4	6.28 \pm 0.12	6.11 \pm 0.1	6.06 \pm 0.06	0.4	6.65 \pm 0.03	6.18 \pm 0.2	6.04 \pm 0.05
0.5	5.73 \pm 0.05	5.59 \pm 0.04	5.50 \pm 0.06	TA $_{\parallel}$ [$\xi\xi$ 0]			
TA $_{\perp}$ [ξ 00]				0.05	1.09 \pm 0.04	0.86 \pm 0.03	0.78 \pm 0.03
0.1	1.29 \pm 0.03	1.14 \pm 0.03	1.03 \pm 0.03	0.1	2.26 \pm 0.05	2.05 \pm 0.1	1.88 \pm 0.03
0.2	2.46 \pm 0.05	2.17 \pm 0.03	2.01 \pm 0.03	0.2	4.75 \pm 0.04	4.65 \pm 0.03	4.02 \pm 0.04
0.3	3.32 \pm 0.10	3.03 \pm 0.02	2.9 \pm 0.03	0.33	6.0 \pm 0.02	5.58 \pm 0.04	
0.4	3.78 \pm 0.10	3.64 \pm 0.06	3.5 \pm 0.04	0.4	5.09 \pm 0.02	4.7 \pm 0.02	
0.5	3.82 \pm 0.1	3.73 \pm 0.08	3.65 \pm 0.08	TO $_{\perp}$ [$\xi\xi$ 0]			
LA [ξ 00]				0.1	5.88 \pm 0.04	5.5 \pm 0.02	5.22 \pm 0.04
0.05	1.16 \pm 0.03	1.05 \pm 0.03	1.02 \pm 0.02	0.2	5.9 \pm 0.02	5.35 \pm 0.02	5.14 \pm 0.1
0.1	2.45 \pm 0.1	2.25 \pm 0.06	2.09 \pm 0.04	0.3	5.44 \pm 0.02	5.02 \pm 0.02	4.76 \pm 0.12
0.2	4.45 \pm 0.1	4.19 \pm 0.04	4.0 \pm 0.04	0.4	4.5 \pm 0.04	4.34 \pm 0.1	4.23 \pm 0.1
0.3	5.8 \pm 0.10	5.50 \pm 0.08	5.58 \pm 0.08	TO $_{\parallel}$ [$\xi\xi$ 0]			
0.4	6.58 \pm 0.2	...		0.1	5.41 \pm 0.04	4.95 \pm 0.06	4.83 \pm 0.04
0.5	7.1 \pm 0.06	6.72 \pm 0.12		0.15	6.03 \pm 0.06	5.87 \pm 0.25	5.3 \pm 0.03
TA $_{\parallel}$ [ξ 00]				0.2	6.6 \pm 0.04	6.2 \pm 0.08	
0.1	1.13 \pm 0.03	0.9 \pm 0.04	0.77 \pm 0.02	0.25	6.9 \pm 0.03		
0.2	2.12 \pm 0.02	1.78 \pm 0.04	1.63 \pm 0.03	0.3	7.1 \pm 0.2		
0.3	2.83 \pm 0.04	2.55 \pm 0.03	2.35 \pm 0.03	0.33	7.01 \pm 0.04	6.87 \pm 0.06	6.84 \pm 0.1
0.4	3.15 \pm 0.03	3.07 \pm 0.06	3.00 \pm 0.03	LO [$\xi\xi$ 0]			
0.5	3.4 \pm 0.04	3.2 \pm 0.08	3.1 \pm 0.05	0.1	5.73 \pm 0.1	5.3 \pm 0.04	4.78 \pm 0.06
TO $_{\perp}$ [ξ 00]				0.2	7.3 \pm 0.1		
0.1	5.5 \pm 0.2	6.17 \pm 0.15	6.3 \pm 0.12	0.3	6.59 \pm 0.1	6.42 \pm 0.1	
0.2	5.62 \pm 0.15	6.10 \pm 0.10	6.20 \pm 0.15	0.4	6.6 \pm 0.1		
0.3	5.86 \pm 0.15	6.05 \pm 0.15	6.25 \pm 0.12				
0.4	6.12 \pm 0.12	6.07 \pm 0.12	6.02 \pm 0.15				
0.5	6.06 \pm 0.15	5.96 \pm 0.15	5.94 \pm 0.12				

dependence of the phonon frequencies. Some insight into the origin of these rather large frequency shifts can be obtained by examining the behavior of the normal modes in the elastic limit. Measurements of the temperature dependence of the elastic constants of Ti have been performed⁶ and show that the decrease in the frequencies with increasing temperature near $q=0$ is much more pronounced for some branches than that observed in the present experiment for the finite wave-vector vibrational modes. This implies that the shifts in the phonon frequencies are related to changes in the long-range interatomic forces which are mainly determined by the detailed electronic response to the nuclear motions. This suggests that the temperature dependence of the normal vibrational modes is closely related to the electronic structure near the Fermi level, since electronic states near the Fermi level play a dominant role in screening the nuclear motions and it is just these states which are strongly affected by changes in temperature.

The most interesting feature of the data is the anomalous temperature dependence of the [001]LO branch. The zone-center mode of this branch softens significantly as the temperature decreases

(Fig. 2), and at room temperature this branch exhibits a dip at the zone center. The behavior of this mode is similar to that observed in hcp Zr (Fig. 3), and thus it seems to be characteristic of the transition metals of column IV of the Periodic Table.

As in the case of hcp Zr we did not observe in the present experiment any dramatic changes in the phonon widths or frequencies as the hcp \rightarrow bcc transformation temperature was approached from below. This suggests that the hcp \rightarrow bcc transition in Ti, as in Zr, is of the first order. This is what one would expect since the hcp \rightarrow bcc transformation in these metals is generally believed to be of the martensitic variety.

Thus the general features of the lattice dynamics of hcp Ti bear a striking resemblance to those of hcp Zr. Actually the measured frequencies for these metals scale approximately by the same factor that one estimates using the Lindemann homology rule,⁷ which takes into account only the difference in atomic mass, lattice spacing, and melting temperature of these metals. This is not surprising in view of the similarity of many of the other properties of these transition elements. Actually de Haas-van Alphen measurements⁸ and a recent band-theoretical calculation⁹ indicate that the electronic structure of Ti is very similar to that of Zr.

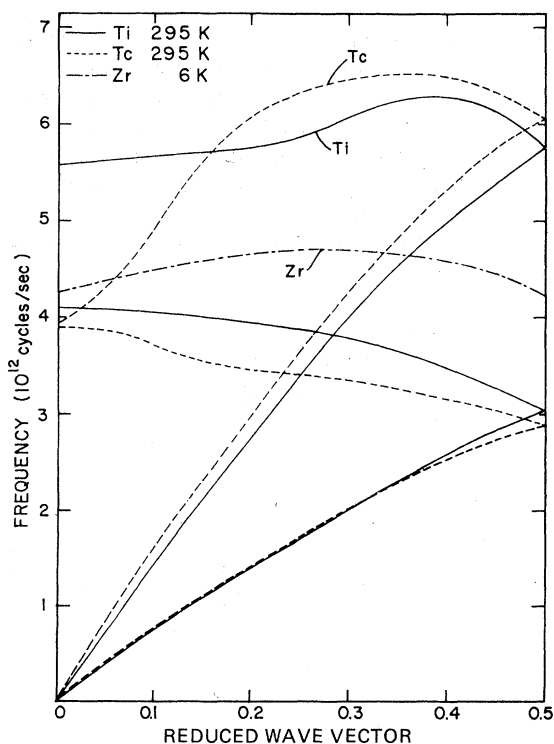


FIG. 3. Comparison of the c-axis dispersion curves of Ti, Zr, and Tc.

B. Lattice specific heat

Under quite general assumptions, which are satisfied in most cases of practical interest, it can be shown¹⁰ that the lattice specific heat at constant pressure $C_p^{(l)}$ can be evaluated starting from the usual harmonic expression for the entropy in which the frequencies are those determined by inelastic neutron scattering. Thus in order to evaluate the specific heat at constant pressure the frequencies and their temperature derivatives are needed at each temperature. Since the frequencies have been determined only at a few temperatures an appropriate interpolation scheme is required to evaluate the temperature derivatives of the frequencies. In I and the present work the interpolation scheme of Miiller and Brockhouse,¹¹ used in their calculations of the thermodynamic properties of Cu and Pd has been adopted. Since this method has been described in considerable detail in the paper of Miiller and Brockhouse as well as in I, only a brief outline of the calculations will be presented here.

Since the experimental frequencies vary to a good approximation linearly with temperature (Fig. 4), the following temperature dependence of the phonon frequencies is assumed:

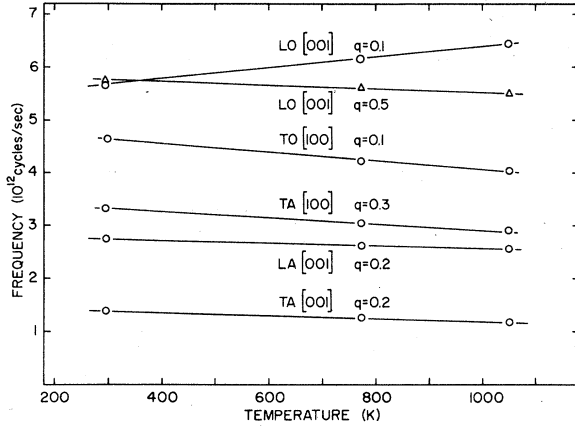


FIG. 4. Temperature dependence of the frequencies of some normal modes of hcp Ti.

$$\omega_{\sigma}(T) = \omega_{\sigma}(T_1)[1 - A(T - T_1)] \equiv \omega_{\sigma}(T_1)f(T), \quad (1)$$

where $T_1 = 295$ K is an appropriate reference temperature, σ stands for (\vec{q}, j) , the wave vector and branch index of the modes, and the constant A is determined from the experimentally measured frequencies. With this assumption the lattice specific heat as a function of temperature can be evaluated using the frequency spectrum at room temperature, $g(\omega, T_1)$,

$$C_p^{(1)} = 3Nk \left(1 - T \frac{f'(T)}{f(T)} \right) \times \int g(\omega, T_1) \frac{x^2}{\sinh^2[xf(T)]} d\omega, \quad (2)$$

where $x = \hbar\omega/2kT$. The frequency spectrum is usually determined by first fitting the data to a Born-von Kármán model and then using the force constants to evaluate the frequencies throughout the appropriate section of the Brillouin zone.

In the present work the data were fitted using the modified axially symmetric model of DeWames *et al.*¹² As it can be seen from Fig. 1 this model provides a satisfactory fit to the experimentally determined dispersion curves. The force constants for the room-temperature data are listed in Table II. Using these force constants, the frequency distribution at room temperature was calculated by the interpolation method of Raubenheimer and Gilat¹³ and it is plotted in Fig. 5. This frequency distribution, together with $f(T)$, were then used in Eq. (2) to evaluate the lattice specific heat as a function of temperature. The validity of the interpolation scheme of Miiller and Brockhouse, used in the present analysis, was carefully examined.

TABLE II. Force constants (10^3 dyn cm) obtained by fitting the 295-K data of hcp Ti to the DeWames *et al.* (Ref. 12) model. These force constants were utilized to obtain the room temperature frequency distribution (Fig. 5) by the interpolation method of Raubenheimer and Gilat (Ref. 13). The notation is that of DeWames *et al.* (Ref. 12).

$K(1, 1-2)$	41.38
$C_{BX}(1, 1-2)$	-3.03
$C_{BZ}(1, 1-2)$	-17.21
$K(2, 1-1)$	22.28
$C_{BX}(2, 1-1)$	0.171
$C_{BZ}(2, 1-1)$	3.78
$K(3, 1-2)$	-8.33
$C_{BX}(3, 1-2)$	1.10
$C_{BZ}(3, 1-2)$	0.22
$K(4, 1-1) + C_{BZ}(4, 1-1)$	12.20
$C_{BX}(4, 1-1)$	0.68
$K(5, 1-2)$	2.26
$C_{BX}(5, 1-2)$	0.17
$C_{BZ}(6, 1-2)$	0.02
$K(6, 1-1)$	0.65
$C_{BX}(6, 1-1)$	1.51
$C_{BZ}(6, 1-1)$	0.23

In particular the entropy at 295, 773, and 1054 K was directly evaluated using the experimentally determined frequency distributions at these temperatures, and it was found to agree to within a few percent with the entropy values obtained using the interpolation scheme of Miiller and Brockhouse (for more details see I).

The calculated lattice specific heat $C_p^{(1)}$ is com-

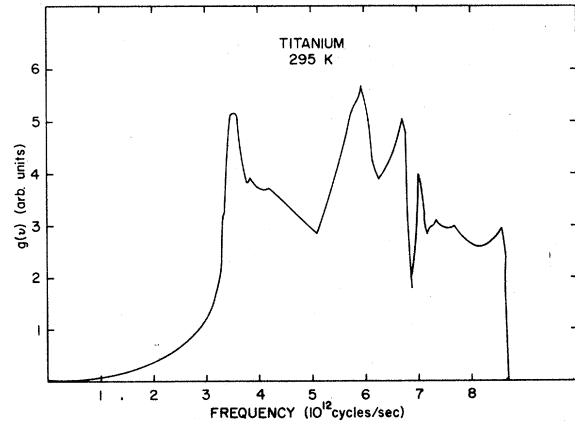


FIG. 5. Phonon spectrum of hcp Ti at 295 K.

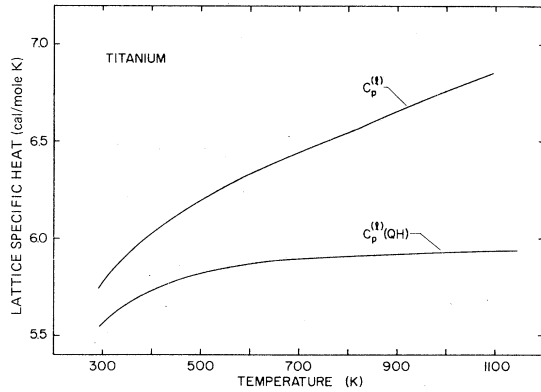


FIG. 6. Temperature dependence of the lattice specific heat at constant pressure $C_p^{(l)}$. $C_p^{(l)(QH)}$ is the quasi-harmonic lattice specific heat given by the first term of Eq. (2).

pared in Fig. 6 with the quasiharmonic lattice specific heat $C_p^{(l)(QH)}$ [given by the first term of Eq. (2)], which of course approaches the classical value at high temperatures. It can be seen that there is a large contribution to the lattice specific heat arising from the explicit temperature dependence of the phonon frequencies given by the second term of Eq. (2). To compare with the experimental total specific heat of the solid C_p , the electronic contribution to the specific heat must be taken into account. The electronic contribution to the specific heat was evaluated using the electronic density of states obtained by Jepsen in its recent band-theoretical calculation⁹ of the electronic structure of Ti. The use of the bare density of states to calculate the

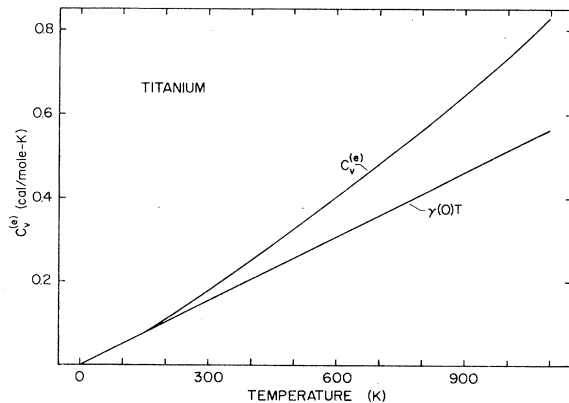


FIG. 7. Electronic contribution to the specific heat $C_v^{(e)}$ evaluated using the electronic density of states obtained by Jepsen (Ref. 9.). $\gamma(0)T$ is the linear extrapolation from low temperatures.

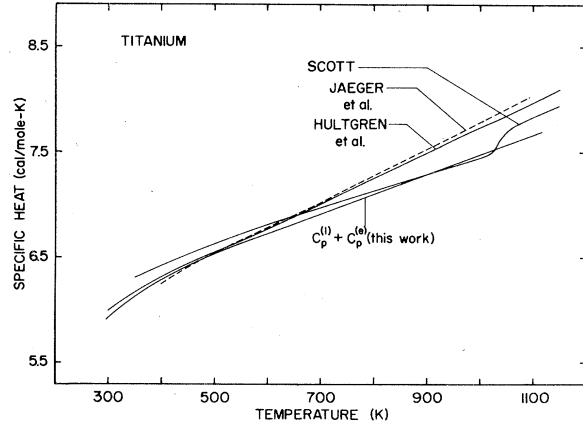


FIG. 8. Comparison of the specific heat at constant pressure C_p obtained by adding $C_p^{(e)}$ to $C_p^{(l)}$ with the experimental results obtained by various workers (Refs. 2, 15, and 16).

electronic specific heat should be valid at high temperatures since the electron-phonon mass enhancement is negligible¹⁴ at temperatures higher than about twice the Debye temperature. It can be seen (Fig. 7) that the calculated electronic specific heat $C_v^{(e)}$ is considerably larger at high temperatures than that obtained by linear extrapolation from low temperatures. In fact the high-temperature electronic specific heat corresponds to an effective density of states at the Fermi level 30% larger than the $T=0$ value of 11.7 states/atom-Ry. This is due to the increase with increasing temperature of the effective electronic density of states at the Fermi level. The total specific heat, obtained by adding the electronic contribution to the lattice specific heat, is compared in Fig. 8 with experimental measurements by various workers^{2,15,16} of the total specific heat of Ti. The agreement is quite satisfactory in view of the large discrepancies in the value reported by various workers for the total specific heat. Thus the observed temperature dependence of the specific heat at high temperatures can be accounted for by the temperature dependence of the lattice and electronic specific heats.

IV. CONCLUSIONS

The lattice dynamics of Ti bear a striking resemblance to that of Zr studied in I. This is not surprising in view of the similarity of their electronic structures as well as many of the other properties of these metals. Since many of the physical properties and in particular the electronic structure¹⁷ of Hf are similar to those of Zr and

Ti, the following general features of the phonon spectra of Zr and Ti are probably characteristic of the transition metals of column IV of the Periodic Table.

(i) The frequencies of all but the [001]LO branch decrease with increasing temperature more than one would expect from the usual effect on the vibrational frequencies of the thermal expansion of the lattice. The contribution to the specific heat arising from this explicit temperature dependence of the normal modes (together with the electronic contribution) explain the general high-temperature features of the measured specific heat.

(ii) The zone-center mode of the [001]LO branch softens appreciably with decreasing temperature and this branch exhibits a dip at the zone center, at room temperature in Ti and at 5.5 K in Zr. It is interesting to note (Fig. 3) that the [001]LO branch of technetium,¹⁸ which has the highest superconducting transition temperature ($T_c \sim 8$ K) of the hcp elements also exhibits a pronounced dip at the zone center (actually the LO and TO have to within experimental errors the same frequency, a degeneracy which is not required by symmetry). Thus, it is tempting to associate the anomalous behavior of this mode with the superconducting properties of the hcp transition elements.

A more fundamental understanding of these experimental results and their relation to the detailed electronic structure of these metals could be obtained only within the framework of the microscopic theory of lattice dynamics.¹⁹ However, in the present stage of development of this theory, no realistic calculations at finite temperatures have been attempted. In I we proposed a qualitative explanation of the experimental results based on the electronic structure of these metals. In order to make a more quantitative assessment of the electronic contribution to the phonon energies we have initiated band structure calculations for the hcp lattice in which the nuclei have been frozen in the positions (furthest from equilibrium) obtained by the zone center longitudinal optic phonon. The qualitative discussion given below is based on our initial calculations, and a much more complete description will be published elsewhere.

The electronic density of states (DOS) of these metals (see I and Ref. 10) exhibits a large peak just above E_F arising from bands of predominantly

d character and a small peak just below E_F arising from the bands near H which contain a large p and d -character admixture. As the temperature increases the effective density of states at the Fermi level increases due to the large d -like peak in the DOS just above E_F . This can be seen directly in the calculated electronic heat capacity which rises above the straight line $[\gamma(T=0)T]$ expected from a constant DOS. This overall increase in the effective DOS will add to the usual metallic screening of the bare Coulomb interaction between ions and leads to a general decrease in the phonon frequencies.

The anomalous behavior of the [001]LO branch near $q=0$ is easier to understand from the reciprocal space (band structure) rather than the real space point of view which we adopted in I. On the AHL plane the bands are doubly degenerate (except for a very small spin-orbit splitting). With a phonon present the symmetry of the lattice is lowered and in general the degeneracies are split. The largest splitting for states on the AHL plane is caused by the [001]LO phonon. The results of our frozen phonon calculations suggest that the bands near H are split at the Fermi level. The band which is lowered in energy remains occupied while the other band is raised above the Fermi level and becomes unoccupied. The net result is a substantial decrease (of the order of a few meV) of the total energy associated with the [001]LO phonon. The splitting is on the order of 1500 K so that as the temperature is raised the thermal repopulation and the thermal disorder wipe out the energy gained by splitting the bands about the Fermi level. The idea that the bands near the Fermi level give rise to the phonon anomalies in this manner is consistent with the recent theoretical work of Varma and Weber,²⁰ and we are presently investigating the detailed connection of our results with their model.

ACKNOWLEDGMENTS

This work was supported by the U. S. Department of Energy, Office of Basic Energy Sciences, Materials Sciences Division. The authors are grateful to O. D. McMasters for providing the single crystals used in the present work.

¹J. H. Mooij, Phys. Status Solidi A 17, 521 (1973); L. P. Filippow, Int. J. Heat Mass Transfer 16, 865 (1973).

²See, for instance, R. Hultgren, P. D. Desai, D. T. Hawkins, M. Gleiser, K. K. Kelley, and D. D. Wagman, Selected Values of the Thermodynamic Proper-

ties of the Elements ASM (1967) (unpublished), and references therein.

³C. Stassis, J. Zarestky, D. Arch, O. D. McMasters, and B. N. Harmon, Phys. Rev. B 18, 2632 (1978).

⁴Thermophysical Properties of Matter, Vol. 12, Ther-

- mal Expansion*, edited by Y. S. Touloukian, R. K. Kirby, R. E. Taylor, and P. D. Desai (IFI/Plenum, New York, 1975), and references therein.
- ⁵R. Ramji Rao and C. S. Menon Phys. Rev. B 7, 644 (1973).
- ⁶E. S. Fisher and C. J. Renken, Phys. Rev. 135, A482 (1964).
- ⁷See, for instance, N. F. Mott and H. Jones, *The Theory of the Properties of Metals and Alloys* (Oxford U.P., London, 1936).
- ⁸G. N. Kamm and J. R. Anderson, *Low Temperature Physics* (Plenum, New York, 1974), Vol. 4; P. M. Everett, Phys. Rev. B 6, 3559 (1972).
- ⁹O. Jepsen, Phys. Rev. B 12, 2988 (1975).
- ¹⁰J. C. K. Hui and P. B. Allen, J. Phys. C 8, 2923 (1975).
- ¹¹A. P. Miiller and B. N. Brockhouse, Can. J. Phys. 49, 704 (1971).
- ¹²R. E. DeWames, T. Wolfram, and G. W. Lehman, Phys. Rev. 138, A717 (1965).
- ¹³L. J. Raubenheimer and G. Gilat, Phys. Rev. 157, 586 (1967).
- ¹⁴G. Grimvall, Phys. Chem. Solids 29, 1221 (1968).
- ¹⁵J. L. Scott, Oak Ridge National Laboratory (ORNL-2328) 1957 (unpublished).
- ¹⁶F. M. Jaeger, E. Rosenbohm, and R. Fonteyne, Rec. Trav. Chim. 55, 615 (1936).
- ¹⁷O. Jepsen, O. K. Andersen, and A. R. Mackintosh, Phys. Rev. B 12, 3084 (1975).
- ¹⁸H. G. Smith, N. Wakabayashi, R. M. Nicklow, and S. Mihailovich, *Proceedings of the Thirteenth International Conference on Low Temperature Physics*, Vol. 3, edited by K. D. Timmerhaus, W. J. O'Sullivan, and E. F. Hammel (Plenum, New York, 1974).
- ¹⁹See, for instance, S. K. Sinha, *Dynamical Properties of Solids*, Vol. 3, edited by G. K. Horton and A. A. Maradudin (North-Holland, Amsterdam, to be published).
- ²⁰C. M. Varma and W. Weber, Phys. Rev. Lett. 39, 1094 (1977).